DE GRUYTER DOI 10.1515/htmp-2012-0103 — High Temp. Mater. Proc. 2012; 31(4-5): 657–665

Evgueni Jak, Peter Hayes*

The Use of Thermodynamic Modeling to Examine Alkali Recirculation in the Iron Blast Furnace#

Abstract: It is widely recognized that alkali metals, such as, potassium and sodium can cause operational problems in the iron blast furnace. These elements can influence properties, such as, the softening and melting of ores, formation of scaffolds, coke properties, and refractory life. It has been established that recirculation of these elements occurs within the furnace. In the lower furnace vaporization occurs in the high temperature hearth and bosch regions, and condensation occurs in the upper furnace below or in the cohesive zone. For these reasons the input of alkalis into the furnace is strictly controlled.

Optimized thermodynamic databases describing slags in the system Al_2O_3-CaO-FeO-Fe_2O_3-Na_2O-K_2O-MgO-SiO_2 have been developed and, combined with the computer software FactSage; these databases have been used to predict the possible behaviour of alkalis in the blast furnace and to examine the effects of changing process variables on reactor performance. To demonstrate this approach to process modeling the furnace is considered as a two-stage equilibrium reaction system and the results of initial analysis are reported.

Keywords: iron blast furnace, slags, alkalis, process modelling

PACS® (2010). 81.05.Bx

Evgueni Jak: Pyrometallurgy Research Centre, The University of Queensland, Brisbane, Australia
***Corresponding author: Peter Hayes:** Pyrometallurgy Research Centre, The University of Queensland, Brisbane, Australia
E-mail: P.Hayes@.uq.edu.au

1 Introduction

The iron blast furnace remains the principal technology used for the production of primary iron because of its inherent chemical and thermal efficiencies. For this reason the process has been extensively studied from the point of view of engineering practice, and with the advent of improved computer technology significant advances have been made in the development of mathematical models that describe the physical processes, e.g. gas flow and burden distribution, occurring within the furnace [1, 2]. There remain aspects of the chemical processes that could be better described but progress to date has been limited in some cases because of the lack of adequate thermodynamic or kinetic models. The behaviour of alkalis in the blast furnace is one of these areas in which modern theoretical tools can now be brought to bear to provide an improved understanding of the process and the implications for industrial practice.

The presence of alkali metals, such as, potassium and sodium, in the iron blast furnace have been reported [3–5] to effect a number of aspects of furnace operation

a. Slagging of blast furnace and stove refractories
b. Formation of scaffolds on the inner walls of the furnace shaft
c. Increased reactivity and degradation of coke
d. Swelling of ore pellets
e. Softening of the iron burden
f. Changes to optimum flame temperature, oxygen enrichment
g. Changes to optimum slag composition

For the most part the effects of increased alkalis are detrimental to furnace productivity and for these reasons the input of alkalis into the furnace is strictly controlled.

Detailed examination of materials obtained from excavations of a number of iron blast furnaces [1] has shown that during operation there is uneven distribution of alkalis in the burden. The concentration of alkalis in both ore and coke are typically greater in the upper furnace and the cohesive zone, indicating that the circulation occurs between the tuyere level and higher levels within the burden.

According to [6] in the upper furnace alkalis are present in the condensed phases principally as carbonates, in the lower furnace in the lower part of the cohesive zone just before melting, as silicates. [7] also report that alkalis are present in burden materials in the cohesive

1st presented Japan-Australia-China Workshop on Iron and Steelmaking, Kyoto, Japan, April 2008, Chairperson Prof M. Iwase.

zone in the form of stoichiometric compounds, such as, kalsilite $K_2O.Al_2O_3.2SiO_2$, melilite and liquid silicate phases

The transport of alkalis between the hearth and cohesive zone, and lower to upper furnace is thought to occur via the formation of gaseous alkali species, e.g., K(g), KCN(g), KF(g) [4, 6, 8]. These gaseous species are formed in the high temperature regions of the furnace, and are condensed or react with the burden or gas species at lower temperatures.

It is now recognised that behaviour of materials in the cohesive zone and control of the softening of the ore burden is an important method of improving bed permeability and furnace productivity. Maximising the volume of the lumpy zone has the effect of improving gas utilisation, and decreasing gas pressure losses thereby increasing furnace productivity. The increased softening and melting temperatures of the burden also have beneficial effects in reducing overall fuel rate and silicon in metal [9].

In the future it is projected that the quality of iron ores will continue to decline with increased alumina and alkali levels depending on the source of raw materials. These impurities are likely to be in the form of smectite clays and other minerals having with them associated potassium.

There are a number of effects on slag behaviour associated with these increased impurity levels. In selecting feed stocks for the furnace upper limits are placed on alumina and alkali levels in the resulting hearth slags based on the effects of individual components. The reality is, however, more complex because of the well established synergistic effects between aluminium and alkali, and alkali earth elements. In the liquid slag structure aluminium 3+ ions are known to replace silicon 4+ ions in the tetrahedral positions provided additional charge can be supplied, this can be achieved in the presence of alkali 1+ ions. This effect is similar to that observed in the formation of 3D feldspar minerals structures. This strong interaction of alkalis with aluminium ions is potentially important to shaft furnace operation in two principle respects.

1. The chemical interaction with aluminium has the effect of lowering the activity of the alkali species in the slags – this makes vapourisation of the alkalis more difficult and has the potential to reduce alkali recirculation. This then is a benefit to the operation.
2. The incorporation of aluminium ions in the tetrahedral positions has the potential to increase rather than decrease slag viscosity, thereby increasing difficulties in slag tapping. This potentially could lead to the need for higher tapping temperatures.

Since the alkalis generate competing and opposite outcomes for the process these complex effects associated with the presence of alumina and alkalis can only quantified and assessed with the development of be predictive models, in this way optimum ore blends for future practice can be identified.

The aim of the study is to demonstrate the application of thermodynamically-based process models to staged chemical reaction systems. The specific objective is to provide a quantitative description of the behaviour of alkalis in the iron blast furnace, the phases that are formed and their chemical compositions, the partitioning of major elements between output streams, and the recirculation of volatile elements; this combined with enthalpy changes within the furnace. Reactions in the gas, solid, slag and metal phases are simultaneously taken into account in the calculations.

2 Description of the two-step iron blast furnace model

The iron blast furnace can be considered as continuous, countercurrent mass and heat transfer reactor in which oxygen is transferred to the ascending gas phase from the descending ore burden, and heat generated by combustion of coke is transferred from the ascending gas phase to the descending condensed phases. The furnace is characterized by a thermal and chemical reserve zone in which gas and condensed phases, under ideal conditions, approach equilibrium. A starting point for the mathematical modeling of the process is to consider the furnace to be described by a series of equilibrium staged processes. To demonstrate this how this can be achieved in the present study the iron blast furnace is described in terms of a simplified two-step model (see Figure 1) consisting of

1. The Hearth Reactor (the high temperature lower furnace), and
2. The Gas Condenser (the cooler upper furnace).

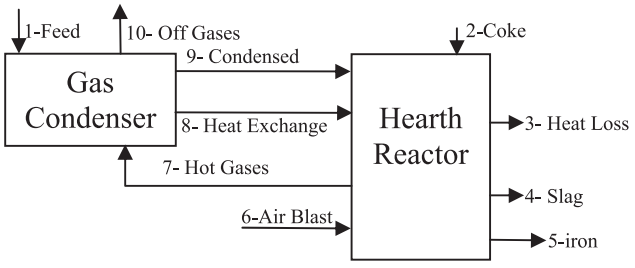

Fig. 1: Two-step iron blast furnace process model.

Coke (stream 2), preheated air blast (stream 6), condensed material (stream 9) and heat exchange enthalpy (stream 8) enter the Hearth Reactor. Equilibrium calculations for the Hearth Reactor predict output streams including compositions and temperature of the slag (stream 4), iron (stream 5) leaving the Blast Furnace, Hot Gases (stream 7) that are passed into the Gas Condenser and Heat loss indicated as stream 3.

Inputs to the Gas Condenser include Fresh feed (stream 1) to the process and Hot Gases (stream 7) from the Hearth Reactor. The equilibrium calculation performed for the Gas Condenser predicts the outcomes of a number of reactions including reduction of feed oxide solids, re-oxidation and condensation of gaseous species passed from the lower furnace. Off gases (stream 10) leave the furnace, and the condensed material (stream 9) and heat exchange enthalpy (stream 8) are passed into the Hearth Reactor.

The calculations are organised in cycles and continued until the mass balance criteria are met, i.e. that the input of volatile elements Na and K in fresh feed (stream 1) equal to the Na and K in output streams including slag (stream 4), iron (stream 5) and off gases (stream 10) within predetermined values (absolute values differ by less than 0.0005%).

The FactSage computer package [10] with a customised thermodynamic database is used for phase equilibria predictions of the phases formed, the compositions of the phases and the partitioning of major elements between the solid compounds, liquid oxide, metal and gas phases in the Hearth Reactor and in the Gas Condenser. In addition to the element and compound databases present in the public domain databases in FactSage, optimized thermodynamic databases describing slags in the system Al_2O_3-CaO-FeO-Fe_2O_3-Na_2O-K_2O-MgO-SiO_2 have been used in the present calculations [11]. The use of these new databases is particularly significant when considering high alkali concentrations and extensive solid solutions that can occur in liquid and solid silicate phases. The model describes heat exchange and associated re-oxidation and condensation reactions in the gas phase during ascending of the gas.

The information on the iron blast furnace used for model development includes major feed stream compositions, stream amounts and stream temperatures. The model output includes the compositions, amounts and temperatures of the off gas, slag, metal streams. A number of assumptions are made:

Metal production	9900 tonnes hot metal (THM)/d
Hearth diam. H_H	14.4 m
Air Blast temperature	1550 K
Coke rate	470 kg/THM
Air blast	1040 Nm^3/THM
Slag mass	320 kg/THM
Alkali load in feed (50%Na_2O/50%K_2O)	10 kg/THM

Table 1: Data on Fukuyama No 5 furnace [12]

The input data for the base case are summarised in Table 1 and are based on data for the Fukuyama No5 blast furnace as reported by [12].

Assumptions:

All iron in feed is 100% fluxed sinter, i.e. all limestone and magnesia-containing minerals are fully calcined to oxides and incorporated in sinter.
50% ($SiO_2 + Al_2O_3$) impurities are in sinter, 50% in coke, at the same Al_2O_3/SiO_2 ratios.
All flux materials CaO, MgO as oxides.
All impurities SiO_2, Al_2O_3, Na_2O, K_2O as oxides.
S is not considered in the calculations.
Lower furnace Hearth Temperature = slag and metal tapping temperature, 1800 K.

For the calculations reported in the present paper the following parameters have been varied: Alkali loading; Slag basicity, CaO/SiO_2; Hearth temperature. Details of the combinations of conditions considered are summarized in Table 3.

In practice the total gas pressure within the furnace also changes with height and position; in the present calculations the total pressure is assumed to be 2 atm. in the Hearth Reactor and 1 atm. in the Gas Condenser, reflecting the pressure drop across the packed bed of the furnace.

For the Gas Condenser, all gas species and most of the solid and liquid stoichiometric species were selected. Importantly, graphite and Fe_3C were excluded from possible

SiO_2	CaO	MgO	Al_2O_3	Al_2O_3/SiO_2	CaO/SiO_2	Approx. T_{liq}
34.63	41.70	6.74	11.57	0.334	1.20	1700 K

Table 2: Base Slag composition (mass%) [3]

	input	input	input	input	input
Calculation No.	T_{offgas} K	$Na_2O + K_2O$ kg/THM	$Na_2O + K_2O$ t/d	CaO/SiO_2 mass%	T_{hearth} K
1	700	10	99.0	1.20	1800
2	600	10	99.0	1.20	1800
3	600	5	49.5	1.20	1800
4	600	7.5	74.3	1.20	1800
5	600	10	99.0	1.00	1800
6	600	10	99.0	1.40	1800
7	600	10	99.0	1.20	1750
8	600	10	99.0	1.20	1850

Table 3: Summary of blast furnace calculation conditions

products of the Gas Condenser to simulate the metastability of CO and absence of the carbon formation even at high CO concentrations in the upper furnace.

3 Results and discussion

Based on the input and output conditions specified above the predicted effects of changing process variables on the steady state performance of the furnace are calculated. A summary of all input and output data are provided in Table 5.

Table 4 shows a summary of the condensed phases in the Gas Condenser for the base case calculation no 2. It can be seen that the alkalis in the condenser consist principally of solid potassium carbonate and alkali silicate phases, the sodium species appear to be concentrated in the silicate. The alkali-containing gas species present in the Hearth Reactor consist predominantly of elemental K and Na, and the cyanides KCN and NaCN, see Table 5.

Figure 2a–c shows the effect of alkali load on the recirculating alkali load in the furnace. It can be seen that decreasing the alkali in the input leads to an almost linear decreases the recirculating alkali load. It can also be seen from Figure 2a that the recirculation of potassium is approximately an order of magnitude greater than that of sodium; in both cases the % recycling does not change significantly with total load in the range investigated. Despite these effects decreasing the alkali in the input only marginally decreases the concentrations of alkali in the hearth slag in the range of compositions examined (Figure 2b). Increased alkali in the furnace input does have a significant effect on the heat requirements in the Hearth Reactor (Figure 2c); the enthalpy of reactions in the lower furnace becoming increasingly endothermic with increasing alkali loadings. The heat balance between the Hearth Reactor (lower furnace) and the Gas Condenser

Compounds	t/day
$K_2Ca_2(CO_3)_3$	3080
$K_2Ca_3Si_6O_{16}$	851
$NaAlSiO_4$, nepheline-b	672
$K_2FeSi_3O_8$	443
KAlSiO, kaliophilite-hexagonal	415
Mg_2SiO_4, forsterite	399
$CaCO_3$, calcite	181

Table 4: Alkali and alkali earth-containing phases in the Gas Condenser for the base case (No 2, gas exit 600 K)

(upper furnace) is also markedly affected by increasing alkali loading; the calculations shown in (Figure 2c) indicate that at higher alkali loadings this can lead to thermal instability with insufficient heat energy being generated in the hearth to sustain the high alkali circulation and the requirements to preheat the descending burden.

Figures 3a and 3b show the effects of CaO/SiO_2 ratio in the hearth slag on the recirculating alkali load in the furnace and the concentrations of alkali in the hearth slag. Increasing CaO/SiO_2 results in increased recirculating loads and decreases in alkali in the hearth slag. Again increased alkali recirculation is accompanied by increasingly positive enthalpies of reaction in the Hearth Reactor and unfavourable heat balance (Figure 3c).

The effects of increasing hearth temperature on alkali recirculation are shown in Figures 4a and 4b; increase in hearth temperature leads to increased recirculation for both potassium and sodium species. Increasing hearth temperature is accompanied by increasingly positive enthalpies of reaction in the Hearth Reactor and unfavourable heat balances (Figure 4c).

A simplified model of the iron blast furnace has been demonstrated in the present study. Clearly from these calculations useful trends in furnace behaviour can be identified and these are consistent with plant observations,

Condenser gas composition (vol% = mol%)

57.638 vol% N_2	0.18296E-36 vol% SiO
23.217 vol% CO	0.17843E-36 vol% O
19.145 vol% CO_2	0.11615E-36 vol% KO
0.32200E-11 vol% KCN	0.25266E-37 vol% N_3
0.23954E-11 vol% C_3O_2	0.44530E-38 vol% O_2
0.25516E-12 vol% $(CN)_2$	0.94721E-39 vol% Na_2
0.10842E-13 vol% NaCN	0.67619E-39 vol% NaO
0.13507E-15 vol% $Fe(CO)_5$	0.86874E-42 vol% CNN(g)
0.94028E-17 vol% K	0.64401E-42 vol% C_3
0.52852E-17 vol% $(KCN)_2$	0.27624E-43 vol% Ca
0.22928E-19 vol% Na	0.26186E-44 vol% NO_2
0.22828E-19 vol% C_4N_2	0.14614E-45 vol% C_5
0.10953E-19 vol% $(NaCN)_2$	0.50379E-46 vol% MgN
0.35074E-25 vol% NCO	0.77719E-47 vol% C
0.34477E-25 vol% CN	0.57594E-47 vol% MgO
0.31229E-25 vol% NO	0.32420E-50 vol% C_2
0.17629E-25 vol% Fe	0.17027E-50 vol% C_4
0.41859E-26 vol% C_2O	0.23137E-53 vol% CaO
0.35070E-29 vol% N2O	0.14583E-55 vol% AlO
0.29008E-29 vol% C2N	0.11205E-55 vol% Al
0.24235E-32 vol% CNN	0.62233E-57 vol% SiN
0.15291E-32 vol% Mg	0.45529E-61 vol% Si
0.53395E-34 vol% FeO	0.59105E-62 vol% SiC_2
0.86939E-35 vol% K_2	0.58881E-66 vol% AlO_2
0.62250E-36 vol% N	

Hearth Reactor gas composition (vol% = mol%)

53.021 vol% N_2	0.46730E-08 vol% C_3O_2
42.339 vol% CO	0.42479E-08 vol% MgO
2.1409 vol% K	0.26760E-08 vol% Al_2O
1.9374 vol% KCN	0.26390E-08 vol% FeO
0.28979 vol% Na	0.18694E-08 vol% N
0.22069 vol% NaCN	0.80499E-09 vol% SiC_2
0.41337E-01 vol% Mg	0.72117E-09 vol% NaO
0.34469E-02 vol% SiO	0.56169E-09 vol% NCO
0.27651E-02 vol% CO_2	0.51953E-09 vol% C_4N_2
0.16150E-02 vol% $(KCN)_2$	0.39826E-09 vol% AlO
0.95963E-03 vol% Fe	0.12707E-09 vol% CaO
0.43296E-03 vol% K_2	0.79253E-10 vol% O
0.67655E-04 vol% $(NaCN)_2$	0.54042E-10 vol% CNN(g2)
0.51481E-04 vol% Ca	0.14374E-10 vol% Si_2N
0.14118E-04 vol% Na_2	0.12631E-10 vol% C
0.10558E-04 vol% $(CN)_2$	0.10184E-10 vol% C3
0.22305E-05 vol% CN	0.85950E-11 vol% Si_2C
0.33543E-06 vol% Al	0.43994E-12 vol% N_2O
0.29724E-06 vol% MgN	0.30915E-12 vol% C_2
0.55215E-07 vol% Si	0.17119E-12 vol% SiC
0.25302E-07 vol% SiN	0.11920E-12 vol% $(AlO)_2$
0.22207E-07 vol% C_2N	0.11801E-12 vol% Si_2
0.73731E-08 vol% NO	0.53167E-13 vol% N_3
0.71573E-08 vol% C_2O	0.50506E-13 vol% Ca_2
0.58168E-08 vol% Mg_2	0.47089E-13 vol% CNN(g)
0.49788E-08 vol% KO	0.16723E-13 vol% AlN

Table 5: Summary of calculations for base case no 2. (Gas Condenser input temperature 600 K, alkali loading $Na_2O + K_2O$ 10 kg/THM; CaO/SiO_2 1.20 wt%; Reactor Hearth temperature 1800 K)

Hearth Reactor gas composition (vol% = mol%)

0.85959E-14 vol% O_2	0.49980E-18 vol% NO_2
0.59266E-14 vol% AlC	0.12484E-22 vol% $Fe(CO)_5$
0.22057E-14 vol% Al_2	0.22059E-29 vol% O_3
0.36777E-15 vol% C_5	0.15503E-31 vol% NO_3
0.21648E-15 vol% C_4	0.71768E-34 vol% N_2O_3
0.70890E-16 vol% AlO_2	0.54919E-45 vol% N_2O_4
0.98758E-17 vol% Si_3	0.91957E-56 vol% N_2O_5

Table 5: (Cont.)

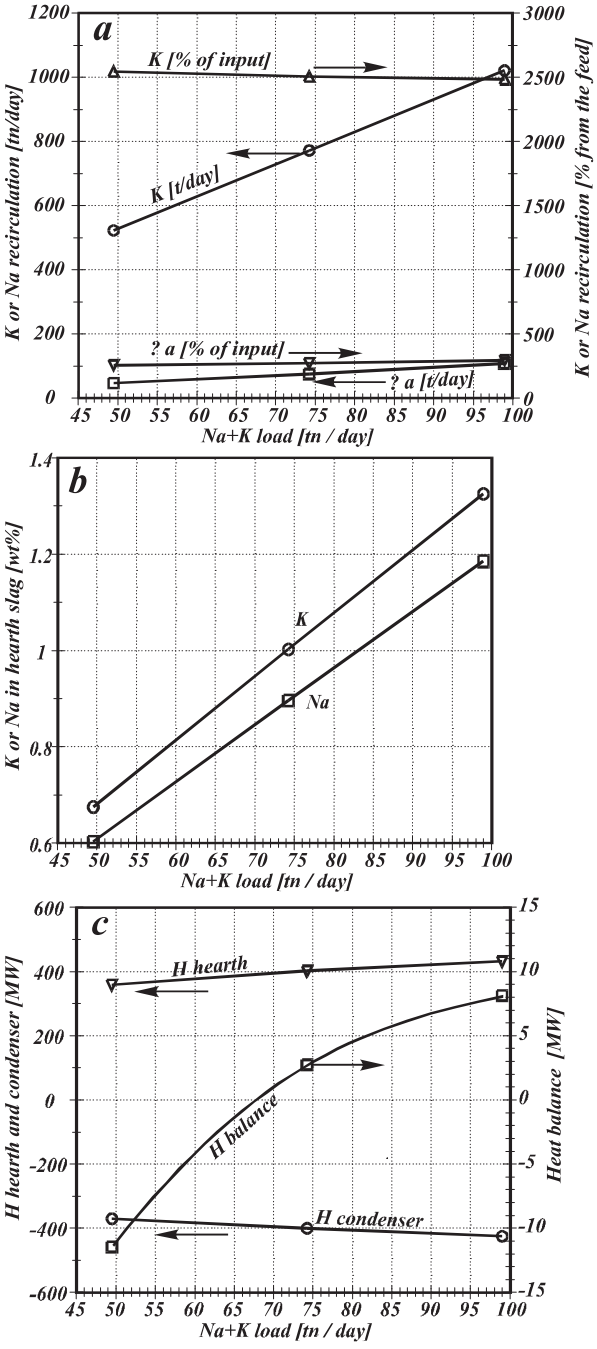

Fig. 2 a–c: Predicted effects of alkali loading on blast furnace performance.

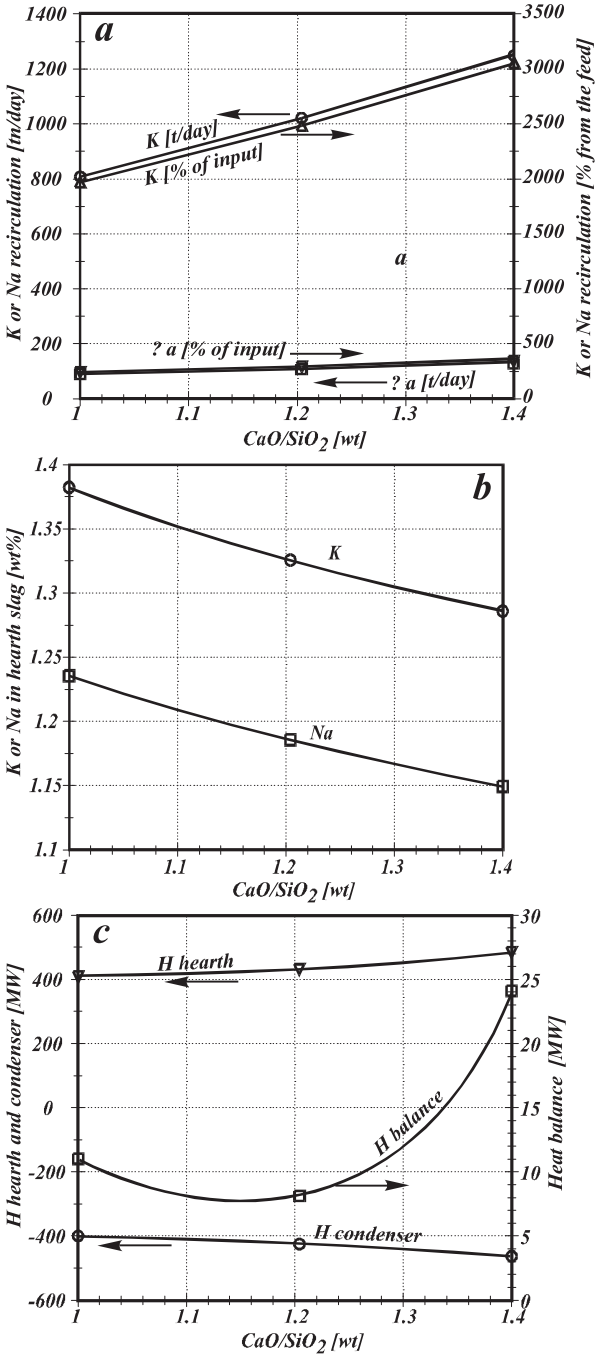

Fig. 3 a–c: Predicted effects of hearth slag CaO/SiO_2 on blast furnace performance.

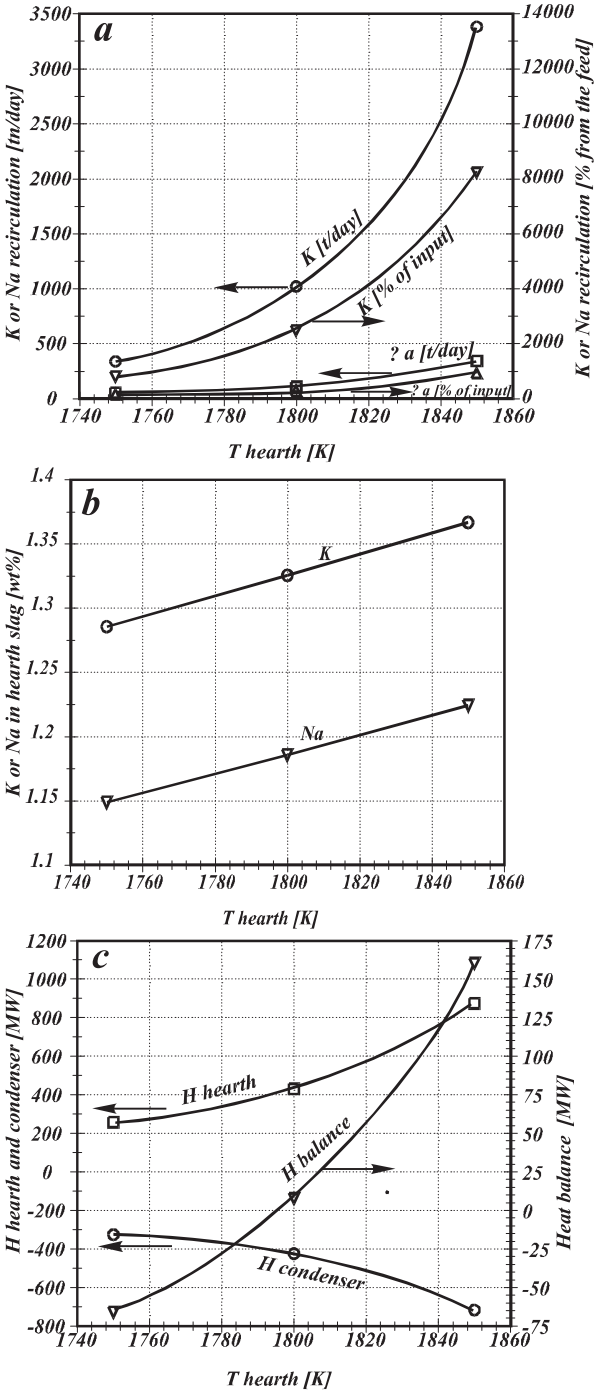

Fig. 4 a–c: Predicted effects of hearth temperature on blast furnace performance

the two-stage model presented here is, however, intended as a demonstration model and the absolute values quoted here should be treated with caution; further refinements and model verification are required before it can be used in forecasting actual practice.

There are number of ways that the model can be refined to improve the accuracy of the predictions and provide further useful information.

Increasing the number of equilibrium steps or condenser stages to correspond with different temperatures will make it possible to calculate the effects in the different regions within the furnace. It has been shown [6, 13], that at different positions within the furnace the alkalis are present in different phases. In the cohesive zone the formation of liquid silicates containing high iron oxide

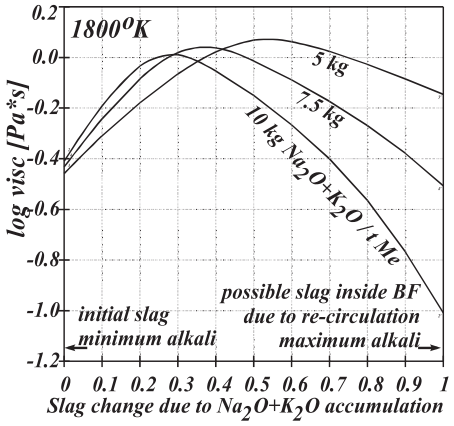

Fig. 5: Possible changes to hearth slag viscosities inside the iron blast furnace due to alkali re-circulation (at 1800 K).

and alkalis are observed; alkali carbonates are reported to be predominant in the upper furnace.

Further refinements of the heat balance in the furnace can be undertaken by including the heat losses through the reactor walls at the different heights in the furnace.

The thermodynamic databases and models in FactSage are also in the process of improvement [14] these will lead to improved accuracy in predictions.

The impact of alkalis on the viscosities of slags can now also be estimated through the development of slag viscosity models [15]. Due to the interaction of alkali and aluminium species in the melt these changes in physico-chemical properties can be complex. Figure 5 shows that at low alkali loadings hearth slag viscosities are increased but at higher concentrations the viscosities decrease with increasing alkali levels.

4 Summary

By considering the iron blast furnace as a series of equilibrium staged processes a mathematical model of the process can be developed that enables mass and energy balances, and the chemical and thermo-chemical equilibria in each stage to be calculated.

It has been shown that optimized thermodynamic databases describing slags in the system Al_2O_3-CaO-FeO-Fe_2O_3-Na_2O-K_2O-MgO-SiO_2, combined with the computer software FactSage can been used to predict the behaviour of alkalis in the blast furnace and to examine the effects of changing process variables. This is a potentially powerful tool for analysis that can be further extended and refined.

Acknowledgements

The development of the new FactSage databases containing Na_2O-K_2O-MgO was supported financially by the Cooperative Research Centre for Coal in Sustainable Development (CCSD) and the Commonwealth Government of Australia.

The authors would like to acknowledge the important contributions made in the field of process metallurgy by Prof Masa Iwase, Kyoto University, and pay tribute to his efforts and encouragement in promoting exchange of scientific ideas and knowledge.

Received: June 13, 2012. Accepted: July 12, 2012.

References

[1] ISIJ, *Blast Furnace Phenomena and Modelling,* Elsevier Applied Science, (1987).
[2] X.F. Dong, A. B. Yu, S. J. Chew and P. Zulli, *Metall. Material. Trans. B*, **41**(2), pp. 330–349 (2010).
[3] N. Standish and W.-K. Lu, *Proc. Symp. Alkalis in the Blast Furnace*, McMaster Univ., Hamilton, Canada, (1973).
[4] A.K. Biswas, *Principles of Blast Furnace Ironmaking – Theory and Practice*, SBA Publications, Calcutta, India, (1981).
[5] A.A. El Geassy, *Trans ISIJ*, **26**, pp. 865–874 (1986).
[6] Q. Zhou and X. Bi, *Scand. J Metall*, **16**, pp. 57–66 (1987).
[7] K. Narita, M. Maekawa and H. Kanayama, *Tetsu-te-Hagane*, **66**, p. 1860 (1980).
[8] W.J. Rankin and J.B. See, *Minerals Sci. Engineering*, **9**(2), pp. 68–82 (1977).
[9] T. Mizyazaki, *Tetsu-te-Hagane*, **67**, pA13 (1981).
[10] FactSage http://www.crct.polymtl.ca
[11] E. Jak and P.C. Hayes, Final report, Prediction of liquidus temperatures and high temperature phase equilibria for the system SiO_2-Al_2O_3-FeO-Fe_2O_3-CaO with addition of Na_2O-K_2O-MgO, *Cooperative Research Centre for Coal in Sustainable Development* (CCSD), Brisbane, Australia, (2004).
[12] J. G. Peacey and W.G. Davenport, *The Iron Blast Furnace – Theory and Practice, Pergamon*, (1979).
[13] O. Ivanov, L. Savov and D. Janke, *Steel Research Intl.*, vol. 75, pp. 443–441, 442–448 (2004).
[14] E. Jak, P. Hayes, A.D. Pelton and S.A. Decterov, *VIII Intl. Conf. Molten Slags and Fluxes, Santiago, Chile, Univ. of Concepcion, (2009)* paper 49.
[15] E. Jak, *VIII Intl. Conf. Molten Slags and Fluxes, Santiago, Chile Univ. of Concepcion (2009)* paper 46.

Appendix

Input

case	input t/day	Fe t/day	Si t/day	Ca t/day	Mg t/day	Al t/day	Na t/day	K t/day	C t/day	O t/day	N t/day
1	32273.59	9405.00	623.92	966.44	131.81	198.57	36.72	41.09	4656.96	6903.78	9309.30
2	32273.59	9405.00	623.92	966.44	131.81	198.57	36.72	41.09	4656.96	6903.78	9309.30
3	32273.59	9405.00	632.39	982.03	133.93	201.78	18.36	20.55	4656.96	6913.30	9309.30
4	32273.61	9405.00	628.16	974.24	132.87	200.17	27.55	30.82	4656.96	6908.55	9309.30
5	32273.60	9405.00	666.31	867.38	142.44	214.61	36.72	41.09	4656.96	6933.79	9309.30
6	32273.59	9405.00	588.82	1048.49	122.99	185.29	36.72	41.09	4656.96	6878.93	9309.30
7	32273.59	9405.00	623.92	966.44	131.81	198.57	36.72	41.09	4656.96	6903.78	9309.30
8	32273.59	9405.00	623.92	966.44	131.81	198.57	36.72	41.09	4656.96	6903.78	9309.30

Iron output

case	mass% input	g-Fe mass%	g-Ca mass%	g-K mass%	g-Si mass%	g-Al mass%	g-Mg mass%	g-Na mass%	g-O mass%	g-N mass%	g-C mass%
1	31.0	94.0	1.3E-05	0	1.34	0.00478	0.00007	0	8.3E-05	0.00754	4.65
2	31.0	94.0	1.3E-05	0	1.32	0.00463	0.00006	0	8.3E-05	0.00748	4.66
3	31.0	93.9	1.3E-05	0	1.57	0.00563	0.00006	0	8.4E-05	0.00774	4.54
4	31.0	93.9	1.3E-05	0	1.43	0.00505	0.00006	0	8.4E-05	0.00758	4.60
5	31.1	93.7	1.0E-05	0	1.89	0.00498	0.00006	0	8.9E-05	0.00769	4.40
6	30.9	94.3	1.6E-05	0	0.86	0.00415	0.00007	0	8.0E-05	0.00718	4.87
7	30.9	94.4	3.4E-06	0	0.86	0.00171	0.00002	0	5.2E-05	0.00708	4.74
8	31.1	93.6	5.0E-05	0	1.76	0.01069	0.00020	0	1.6E-04	0.00728	4.60

Slag output

case	mass% input	Fe mass%	Ca mass%	K mass%	Si mass%	Al mass%	Mg mass%	Na mass%	O mass%	N mass%	C mass%
1	9.6	0.0048	31.2	1.328	15.8	6.4	4.3	1.187	39.7	0	0
2	9.6	0.0049	31.2	1.326	15.9	6.4	4.3	1.186	39.7	0	0
3	9.4	0.0050	32.3	0.675	15.6	6.6	4.4	0.604	39.8	0	0
4	9.5	0.0050	31.7	1.003	15.8	6.5	4.3	0.897	39.8	0	0
5	9.2	0.0052	29.2	1.382	16.0	7.2	4.8	1.235	40.2	0	0
6	9.9	0.0049	32.8	1.286	15.7	5.8	3.8	1.149	39.4	0	0
7	9.9	0.0062	30.2	1.286	16.8	6.2	4.1	1.149	40.2	0	0
8	9.3	0.0044	32.2	1.367	14.9	6.6	4.4	1.224	39.3	0	0

Off gas (from condenser)

	gas% input mass% input	Fe mass%	Ca mass%	K mass%	Si mass%	Al mass%	Mg mass%	Na mass%	O mass%	N mass%	C mass%
1	55.5	1.8E-18	1.7E-35	3.2E-10	1.9E-31	7.9E-47	2.3E-27	1.1E-14	31.7	52.0	16.3
2	55.5	2.4E-16	3.6E-44	4.1E-12	1.7E-37	2.2E-56	1.2E-33	8.0E-15	31.7	52.0	16.4
3	55.1	7.6E-17	2.0E-44	9.6E-13	1.5E-37	2.2E-56	6.9E-34	1.9E-15	32.1	52.4	15.5
4	55.4	1.7E-16	3.0E-44	3.1E-12	1.4E-37	2.1E-56	1.1E-33	6.1E-15	31.8	52.1	16.1
5	55.6	1.8E-16	2.9E-44	3.1E-12	1.4E-37	2.1E-56	1.1E-33	6.0E-15	32.0	51.8	16.2
6	55.8	5.8E-16	4.9E-44	1.1E-11	2.2E-37	2.6E-56	1.8E-33	2.2E-14	31.2	51.7	17.1
7	54.0	1.0E-17	9.8E-45	9.4E-15	2.8E-37	1.2E-55	2.1E-34	1.9E-17	32.2	53.4	14.4
8	58.7	6.9E-15	3.4E-44	5.4E-09	2.6E-37	2.6E-60	2.2E-32	1.1E-09	30.2	49.1	20.7

Gas over hearth reactor [t/day]

case	Fe	Ca	K	Si	Al	Mg	Na	O	N	C
1	0.3	0.0	1003.8	0.6	0.00006	6.3	74.1	4015.6	9308.5	3178.0
2	0.3	0.0	980.3	0.6	0.00006	6.2	72.1	4161.4	9308.6	3283.1
3	0.3	0.0	502.2	0.7	0.00007	5.2	28.9	3962.2	9308.5	3054.9
4	0.3	0.0	741.2	0.6	0.00006	5.6	47.9	4127.7	9308.5	3217.9
5	0.3	0.0	767.8	0.8	0.00006	6.1	53.6	4117.0	9308.5	3214.9
6	0.3	0.0	1212.1	0.4	0.00005	6.4	98.2	4433.8	9308.6	3525.2
7	0.1	0.0	298.6	0.3	0.00001	1.5	19.2	3568.3	9308.6	2728.2
8	0.8	0.1	3343.8	1.1	0.00032	26.7	309.9	5533.6	9460.4	4670.4